Journal of Photochemistry and Photobiology A: Chemistry 202 (2009) 1–9

Contents lists available at ScienceDirect

Journal of Photochemistry and Photobiology A: Chemistry

journal homepage: www.elsevier.com/locate/jphotochem

Structure and photophysical properties of new lanthanide(III) complexes $[Ln(C_{10}H_8O_6)_{1.5}(H_2O)_3]\cdot H_2O$

Paula Gawryszewska*, Zbigniew Ciunik

Faculty of Chemistry, University of Wroclaw, 14 F. Joliot-Curie Str., 50-383 Wroclaw, Poland

ARTICLE INFO

Article history:
Received 6 June 2008
Received in revised form 5 September 2008
Accepted 7 October 2008
Available online 17 November 2008

Keywords:
Terbium
Europium
Luminescence
Charge transfer state
O-Phenylenedioxydicarboxylic acid

ABSTRACT

A serie of lanthanide complexes with o-phenylenedioxydiacetic acid (PDDA) was synthesized and the crystal structure was resolved. The compounds $[Ln(C_{10}H_8O_6)_{1.5}(H_2O)_3]\cdot H_2O$ (where Ln = Tb(III), Gd(III) and Eu(III)), crystallize as polymer with the space group *Pbcn* and $a = 34.075(2)$ Å, $b = 12.595(1)$ Å, $c = 8.314(1)$ Å. Absorption, emission, and excitation spectra at 293 K, 77 K and 4 K as well as luminescence decay time measurements were used to characterize the dynamics of the excited states and to determine the ligand-to-metal energy transfer mechanism for the complexes in solid state and solution. The role of the C–T state in these processes has been analysed. The results are compared with those achieved for a $Na[Eu(C_{10}H_8O_6)_2(H_2O)_2]\cdot 4H_2O$ complex and a Eu(III) complex with PDDA in aqueous solution.

1. Introduction

In recent years great efforts have been undertaken to investigate structure and optical properties of lanthanide complexes, which was due to their potential to be sensitive and selective probes in a wide variety of biological applications [1–7]. The design of efficient luminescent lanthanide-based probes requires a detailed knowledge of the efficiency of the ligand-to-metal energy transfer, solution structure and dynamics and of the influence that these have on important photochemical and photophysical properties [8–17]. The knowledge of radiative (or natural) lifetime of lanthanide complexes with organic ligands is also important [18].

The most emissive lanthanide(III) ions are Tb(III) and Eu(III). These ions emit in the visible region of the spectrum; far removed from the most intrinsic fluorescence of organic or biological molecules. If overlapping luminescence is present, it can usually be easily separated from the lanthanide luminescence by simple time discrimination, since the lifetimes of Eu(III) and Tb(III) are normally on the order of 0.1–2 ms. In order to overcome very small absorption coefficient of the excitation, f–f transitions usually rely on energy transfer from the ligands surrounding the lanthanide ion. The main path of the energy transfer between the excited ligand molecule and the excited Ln(III) states involves the ligand-centred $3\pi\pi^*$ state, but there are many different factors influencing the overall quantum yield of the metal-centred luminescence, e.g. the rate of the intersystem crossing and the rate of the ligand-to-metal energy transfer, the presence of high-energy vibrations deactivating an excited state of the metal ion. The localization of the low-lying ligand-to-metal charge transfer state (LMCT) in relation to the excited states of Eu(III) is very important, since the influence of the LMCT on quenching of the Eu(III) emission is well documented [19–23]. If observation of the LMCT is impossible due to overlap with more intense absorptions of ligands, the LMCT energy can be predicted according to a theoretical model developed by Malta et al. [24]. Recently, a theoretical approach to intramolecular energy transfer through charge transfer state in lanthanide compounds has been developed [25]. However, some authors point to luminescence quenching through the formation of intramolecular excimers between ligand strands [26].

This work presents a detailed study of lanthanide (Tb(III), Gd(III), Eu(III)) complexes with PDDA ($[Ln(C_{10}H_8O_6)_{1.5}(H_2O)_3]\cdot H_2O$) at wide range of temperatures from 4 to 295 K with a view to probing the specific energetic and structural characteristics that influence luminescence efficiency. The work focuses in particular on the role of the LMCT state for the ligand-to-metal energy transfer and luminescence efficiency as well as the relative contribution of the radiative and non-radiative paths to the excited state deactivation. Spectroscopic results of $[Eu(C_{10}H_8O_6)_{1.5}(H_2O)_3]\cdot H_2O$ were compared with those obtained for the earlier investigated complex,

* Corresponding author. Tel.: +48 71 37 57 394; fax: +48 71 375 74 20.
E-mail address: paula@wchuwr.pl (P. Gawryszewska).

1010-6030/$ – see front matter © 2008 Elsevier B.V. All rights reserved.
doi:10.1016/j.jphotochem.2008.10.023

$Na[Eu(C_{10}H_8O_6)_2(H_2O)_2]\cdot 4H_2O$ [21]. The structure's effect on photophysical properties was demonstrated.

2. Experimental

2.1. Preparation of the crystals

The monocrystals of $[Ln(C_{10}H_8O_6)_{1.5}(H_2O)_3]\cdot H_2O$ and $Na[Eu(C_{10}H_8O_6)_2(H_2O)_2]\cdot 4H_2O$ complexes were obtained by crystallization from aqueous solution at pH 4.5 and 6.5, respectively, with $Ln(ClO_4)_3\cdot 8H_2O$:PDDA molar ratio kept at 1:2. Lanthanide perchlorates were prepared from the oxides (Aldrich 99.99%) and PDDA was also purchased from Aldrich.

2.2. X-ray measurement

X-ray data for crystal 1Eu were collected at low temperature using an Oxford Cryosystem device on a Kuma KM4CCD κ-axis diffractometer with graphite-monochromated Mo Kα radiation ($\lambda = 0.71073$ Å). The crystal was positioned at 65 mm from the CCD camera. 612 frames were measured at 0.75° intervals with a counting time of 20 s. Accurate cell parameters were determined and refined by least-squares fit of 6300 strongest reflections. The data was corrected for Lorentz and polarization effects. Analytical absorption correction was also applied. Data reduction and analysis were carried out with the Oxford Diffraction (Poland) programs. The structure was solved by direct methods (program SHELXS97 [27]) and refined by the full-matrix least-squares method on all F^2 data using the SHELXL97 [28] programs. Non-hydrogen atoms were refined with anisotropic displacement parameters; hydrogen atoms from $\Delta\rho$ maps were included. They were refined with isotropic displacement parameters.

Crystallographic data for the structures reported in this paper (excluding structure factors) has been deposited with the Cambridge Crystallographic Data Centre, CCDC no. 706755. Copies of this information may be obtained free of charge from the Director, CCDC, 12 UNION Road, Cambridge 1EZ, UK (fax: 44 1223 336033, e mail: deposit@ccdc.cam.ac.uk or http://www.ccdc.cam.ac.uk.

2.3. Spectroscopic measurements

Absorption measurements were performed using a Cary-Varian 500 spectrophotometer. Emission spectra were measured with a SpectraPro 750 monochromator, equipped with Hamamatsu R928 photomultiplier and 1200 l/mm grating blazed at 500 nm. The 450 W xenon arc lamp was used as an excitation source, coupled with 275 mm excitation monochromator using a 1800 l/mm grating blazed at 250 nm. Excitation spectra have been corrected for the excitation light intensity, while emission spectra were not corrected for the instrument response. The measurements were done at room, 77 K and 4 K temperatures using liquid-N_2 cooled cryostat or Oxford 1204 helium continuous flow cryostat. The corrected emission spectrum at a temperature of 295 K for Eu(III) complex with PDDA in H_2O was measured using SLM AMINCO SPF-500 spectrofluorimeter equipped with a 300 W Xe-lamp.

Luminescence decay curves were recorded using microsecond time-correlated single photon counting option of FLS920 setup (Edinburgh instruments Ltd.). Excitation was provided by μF900 microsecond Xenon flash lamp under computer control with pulses 1.5–3 μs, an average power >60 W up to 100 Hz and the possibility of measuring decays from 400 ns to 10 s. Luminescence decays measurements were performed in multichannel scaling mode requiring TCC900 fast counter PC plug-in Card. PG900 microsecond photomultiplier gating option was used to fix the gate width and gate delay and a Hamamatsu (R928-Hamamatsu) in Peltier Cooled Housing was used as detector. The photomultiplier was switched off for the duration of the exciting light flash, which ensured the removal of super imposing stray and fluorescence light.

Table 1
Crystal data and structure refinement for 1Eu.

Empirical formula	$C_{15}H_{20}EuO_{13}$
Formula weight	560.27
Temperature, K	100(2)
Wavelength, Å	0.71073
Crystal system	Orthorhombic
Space group	*Pbcn*
a, Å	34.075(2)
b, Å	12.595(1)
c, Å	8.314(1)
α, °	90
β, °	90
γ, °	90
Volume, Å^3	3568.1(3)
Z	8
Dc, Mg m^{-3}	2.086
Mu, mm^{-1}	3.589
F(000)	2216
Crystal size, mm	0.13 × 0.16 × 0.18
θ range for data collection, °	3.45–25.00
Ranges of *h*, *k*, *l*	−38 → 40, −14 → 14, −7 → 9
Reflections collected	18788
Independent reflections (R_{int})	3109(0.0492)
Data/parameters	3109/262
Minimum/maximum absorption correction	0.84084/1.56969
S	1.113
Final R1/*wR2* indices ($I > 2\sigma_I$)	0.0364/0.0606
Largest diff. peak/hole, e Å^{-3}	1.430/−1.596

3. Results and discussion

3.1. X-ray analysis

Single-crystal X-ray diffraction data shows that the structure of $[Ln(C_{10}H_8O_6)_{1.5}(H_2O)_3]\cdot H_2O$ (where Ln = Tb(III), Gd(III), Eu(III) hereafter denoted as 1Tb, 1Gd, 1Eu) is orthorhombic with the space group *Pbcn* and $a = 34.075(2)$ Å, $b = 12.595(1)$ Å, $c = 8.314(1)$ Å. The crystallographic data is presented in Table 1. The molecular structure of 1Eu with the numbering scheme for atoms is displayed in Fig. 1. The complexes with Tb(III) and Gd(III) are isostructural with 1Eu. The polymeric structure consisting of tetrameric units sharing edges is shown in Scheme 1. Two independent ligands (denoted as PDDA I and PDDA II) each play different roles. PDDA I creates chelating rings and is additionally bound to the next metal ion. The PDDA II plays only a bridging role between the two lanthanide ions. The Eu(III) ion is nine-coordinate with the primary coordination sphere made up of two PDDA ligands and three water molecules. Two carboxylate oxygen atoms (O1, O5) and two ether oxygen atoms (O3, O4) of PDDA I as well one carboxylate oxygen atom (O7) of PDDA II are involved in europium-ion coordination. The carboxylate oxygen atom (O6) of PDDA I is coordinated to the next metal ion. This carboxylate group of PDDA I acts as an open bidentate bridge forming a bridging network of the type Eu–O–C–O–Eu with the distance between the Eu(III) ions being 6.146 Å. The polymer is created along *c*-axis. Subsequently, the PDDA II coordinates the two adjacent Eu(III) ions by two one bidentate carboxylate groups, where the distance between the Eu(III) ions is 13.960 Å.

The Eu–O bond lengths to the PDDA ligands are in the expected range with the Eu–O(ether) distances being about 0.2 Å longer than the Eu–O(carboxylate) distances. Selected bond lengths and angles are given in Table 2. The shortest Eu–O bond (2.279(4) Å) is associated with the carboxylate oxygen of PDDA II. The Eu–O(water) bonds of 2.427(3) to 3W and 2.502(3) to 1W are also typical with

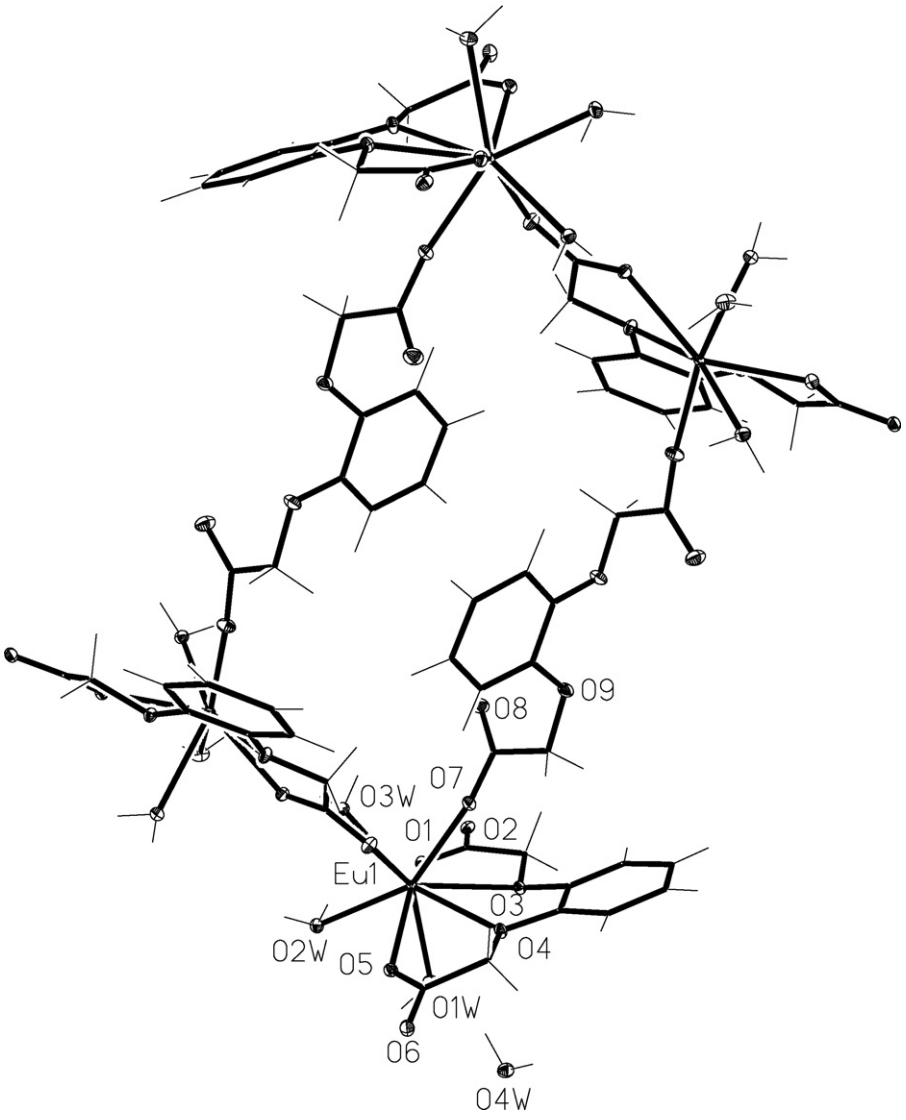

Fig. 1. The X-ray structure of $[Eu(C_{10}H_8O_6)_{1.5}(H_2O)_3]\cdot H_2O$ (1Eu).

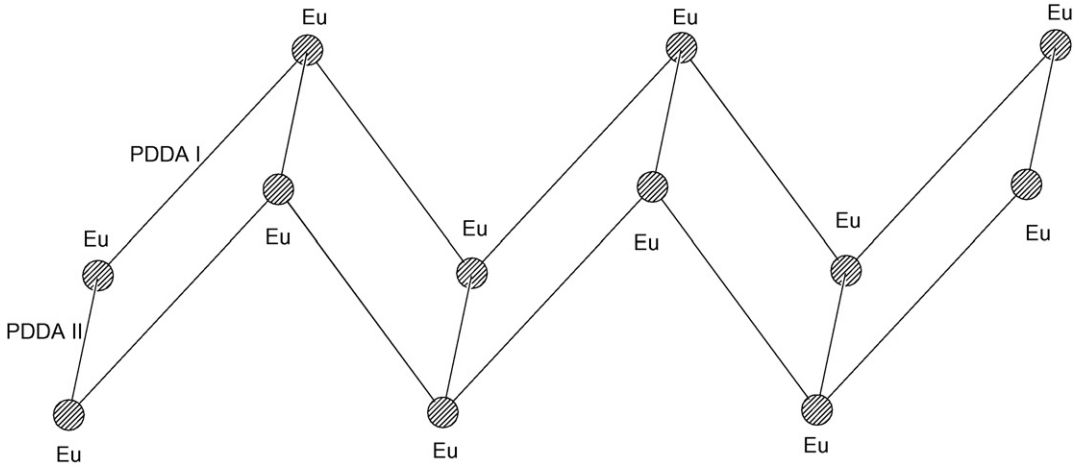

Scheme 1. Polymeric structure of 1Eu.

Table 2
Selected bond lengths (Å) and angles (°) for 1Eu.

Eu(1)–O(7)	2.279(4)
Eu(1)–O(2W)	2.348(3)
Eu(1)–O(1)	2.386(3)
Eu(1)–O(5)	2.403(3)
Eu(1)–O(6)#1	2.407(3)
Eu(1)–O(3W)	2.427(3)
Eu(1)–O(1W)	2.502(3)
Eu(1)–O(4)	2.554(3)
Eu(1)–O(3)	2.650(3)
O(7)–Eu(1)–O(2W)	148.84(12)
O(7)–Eu(1)–O(1)	90.04(13)
O(2W)–Eu(1)–O(1)	88.74(12)
O(7)–Eu(1)–O(5)	124.92(12)
O(2W)–Eu(1)–O(5)	70.01(12)
O(1)–Eu(1)–O(5)	141.19(11)
O(7)–Eu(1)–O(6)#1	74.22(13)
O(2W)–Eu(1)–O(6)#1	87.86(12)
O(1)–Eu(1)–O(6)#1	141.86(12)
O(5)–Eu(1)–O(6)#1	71.55(12)
O(7)–Eu(1)–O(3W)	82.04(12)
O(2W)–Eu(1)–O(3W)	68.75(12)
O(1)–Eu(1)–O(3W)	67.66(11)
O(5)–Eu(1)–O(3W)	127.44(11)
O(6)#1–Eu(1)–O(3W)	75.76(12)
O(7)–Eu(1)–O(1W)	134.35(12)
O(2W)–Eu(1)–O(1W)	74.53(12)
O(1)–Eu(1)–O(1W)	73.07(11)
O(5)–Eu(1)–O(1W)	70.16(11)
O(6)#1–Eu(1)–O(1W)	141.36(12)
O(3W)–Eu(1)–O(1W)	125.71(12)
O(7)–Eu(1)–O(4)	76.22(11)
O(2W)–Eu(1)–O(4)	129.91(11)
O(1)–Eu(1)–O(4)	120.76(11)
O(5)–Eu(1)–O(4)	61.84(11)
O(6)#1–Eu(1)–O(4)	89.51(11)
O(3W)–Eu(1)–O(4)	156.43(11)
O(1W)–Eu(1)–O(4)	77.03(11)
O(7)–Eu(1)–O(3)	65.84(12)
O(2W)–Eu(1)–O(3)	138.34(12)
O(1)–Eu(1)–O(3)	62.51(11)
O(5)–Eu(1)–O(3)	113.24(11)
O(6)#1–Eu(1)–O(3)	133.51(11)
O(3W)–Eu(1)–O(3)	119.16(11)
O(1W)–Eu(1)–O(3)	68.76(11)
O(4)–Eu(1)–O(3)	59.26(10)

Symmetry transformations used to generate equivalent atoms: #1: $x, -y, z-1/2$; #2, $x, -y, z+1/2$; #3, $-x+1, y, -z-1/2$.

the shortest being 2.348(3) (2W). A network of hydrogen bonds stabilizes the structure (see Table 3).

$Na[Eu(C_{10}H_8O_6)_2(H_2O)_2]\cdot 2H_2O$ (denotes 2Eu) is isostructural with the $Na[La(C_{10}H_8O_6)_2(H_2O)_2]\cdot 2H_2O$ complex reported by Choppin and co-workers [29]. 2Eu forms polymeric structure with the space group $\bar{P}1$ and $a = 12.350(3)$ Å, $b = 12.760(2)$ Å, $c = 8.783(2)$ Å, $\alpha = 101.54(2)^\circ$, $\beta = 95.28(2)^\circ$ and $\gamma = 75.98(2)^\circ$. The first coordination sphere of Eu(III) is made up of two independent PDDA ligands and two water molecules (W1, W2). The Eu(III) ion is coordinated by two carboxylate oxygen atoms (O1, O5; O7, O11) and two ether atoms (O3, O4; O9, O10) of each PDDA ligand. The carboxylate oxygen atom, O7, is additionally present in the coordination sphere of both symmetry-related Na(I) ions. Moreover, the carboxylate oxygen atom (O1) and the water molecule (W2) also bridge Na(I) and the Eu(III) ions. The Na(I) is a six-coordinate with two water molecules (W2, W3) and four PDDA carboxylate oxygen atoms (O1, O6, O7, O7*). The bound angles about it are approximately tetrahedral [29].

Table 3
Hydrogen-bonds for 1Eu [Å and °].

D–H···A	d(D–H)	d(H···A)	d(D···A)	<(DHA)
O(1W)–H(1W)···O(1)#4	0.92	1.98	2.902(5)	172.4
O(1W)–H(2W)···O(3W)#4	0.90	2.51	2.997(5)	114.2
O(1W)–H(2W)···O(2)#5	0.90	2.35	3.191(5)	155.7
O(1W)–H(2W)···O(3W)#4	0.90	2.51	2.997(5)	114.2
O(2W)–H(3W)···O(2)#6	0.89	2.02	2.808(5)	147.2
O(2W)–H(4W)···O(6)#1	0.92	2.38	3.299(5)	171.9
O(3W)–H(5W)···O(4W)#7	0.93	1.76	2.659(5)	162.9
O(3W)–H(6W)···O(5)#1	0.90	1.85	2.716(5)	161.1
O(4W)–H(7W)···O(8)#8	0.90	1.78	2.684(5)	174.0
O(4W)–H(8W)···O(1W)	0.92	2.08	2.859(4)	142.6
O(4W)–H(8W)···O(4)	0.92	2.62	3.309(5)	132.3

Symmetry transformations used to generate equivalent atoms: #1, $x, -y, z-1/2$; #2, $x, -y, z+1/2$; #3, $-x+1, y, -z-1/2$; #4, $-x+3/2, -y+1/2, z+1/2$; #5, $x, -y+1, z+1/2$; #6, $-x+3/2, y-1/2, z$; #7, $x, y, z-1$; #8, $x, y, z+1$.

3.2. Spectroscopic results

3.2.1. Tb and Gd complexes

The 1Tb complex shows strong luminescence upon excitation into ligand absorption band at room, 77 and 4 K temperatures, both in the solid state and in aqueous solution. The bands displayed in Fig. 2 correspond with the well known $^5D_4 \rightarrow {}^7F_J$ transitions where $J = 0$–6. Please note that at 4 K the number of the Stark components of f–f transitions is $2J + 1$. The respective band for the $^5D_4 \rightarrow {}^7F_0$ transition is a singlet with maximum at 680.80 nm, which suggests the presence of only one position of the lanthanide ion in the structure. The splitting of the ^7F_J ($J = 1$–6) energetic levels by the crystalline field amounts to 341, 317, 364, 155, 239, 105 cm^{-1} respectively.

The excitation spectra for the 1Tb monocrystal at 295, 77 and 4 K are plotted in Fig. 3. They consist of a broad band arising from the absorption transition to the ligand singlet state and of the f–f transitions of Tb(III). The ligand-to-metal energy transfer is efficient in the 4–295 K temperature range. No ligand phosphorescence could be detected from 1Tb.

The broad band in the excitation spectrum is shifted to lower energies as compared to the respective band in the absorption spectrum. This is due to the fact that the excitation is only effective at the tail of the absorption band of highly absorbing molecule, which is a consequence of the surface quenching phenomenon (see inset in Fig. 3) [30].

Fig. 4 shows the emission and excitation spectra for the 1Gd monocrystals at 77 K. The 1Gd emission spectrum consists of two bands of the ligand origin in the range of 325–430 nm and 440–600 nm with the lower energetic component being a long-lived emission with a lifetime of 2.560 ms (monoexponential). There are two visible inflexions on the phosphorescence band, apart from the maximum at 20153 cm^{-1}, whose energies were determined by the fitting procedure using Gaussian functions. The three peaks are equally separated by the energy (1200 ± 100 cm^{-1}), which corresponds to a vibrational progression typical for the n, π^* emission from aromatic molecules [31].

The lowest emission wavelength of the triplet state was determined as 23,419 cm^{-1} from the phosphorescence spectrum of the Gd complex at 77 K as well as the location (484.4–486.6 nm) and the splitting of the $^5D_4$ level by the crystal field (93 cm^{-1}) from the excitation spectrum of 1Tb at 4 K. The energy gap between the ligand $3\pi\pi^*$ and $^5D_4$ (20,644 cm^{-1}) states is 2775 cm^{-1}, suitably fulfilling the conditions of the phonon assisted resonance. Such value of the energetic gap eliminates the occurrence of the back-energy transfer phenomenon, frequently observed for Tb(III) with organic ligands [21,32]. The energy back transfer from excited Tb(III) ion to the ligand state is observed when the energy difference between the $^5D_4$ level of Tb(III) and the lowest triplet state energy level of the ligand is less than about 1850 cm^{-1} [33].

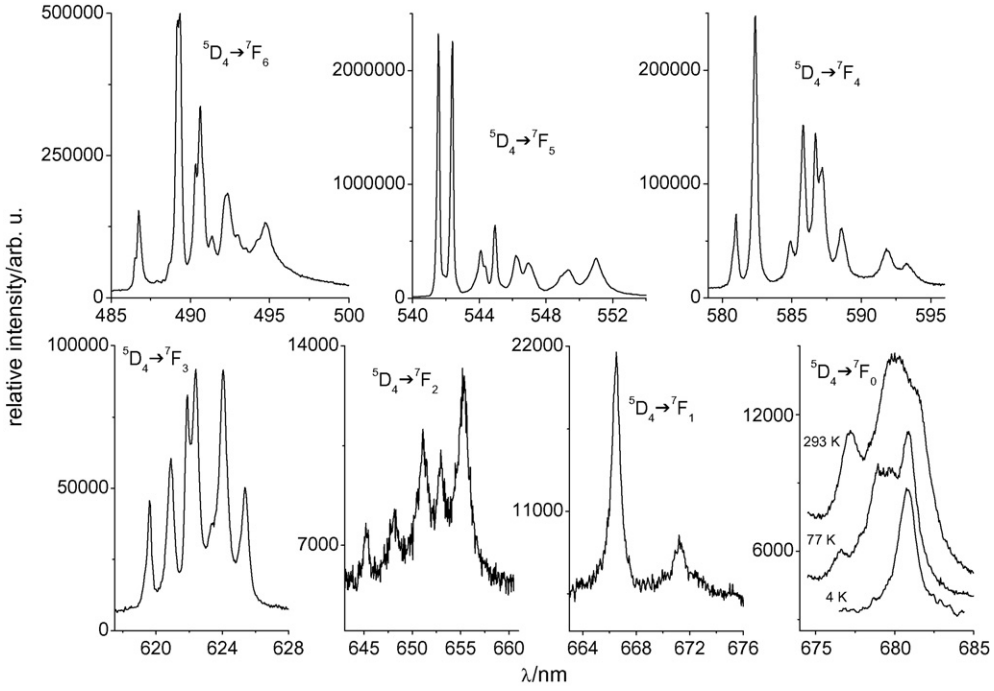

Fig. 2. The luminescence spectra of 1Tb at 295, 77 and 4 K (λ_{exc} = 325 nm).

3.2.2. Eu complexes

Fig. 5 presents the excitation spectrum for the 1Eu monocrystal at 77 K. The spectrum consists only of f–f transition bands corresponding to the transitions from the $^7F_0$ ground state to the excited states of the Eu(III) ion. Similarly as for 2Eu, sensitised emission was not observed in spite of good resonance conditions with respect to the Eu(III) levels ($\Delta E = E_{trip} - E(^5D_2) = 1886\ cm^{-1}$), where an energy transfer ($3\pi\pi^* \rightarrow {}^5D_2$) can occur by the dipole-2^λ pole mechanism [19,25,34].

The LMCT state deactivates the ligand states in 1Eu and 2Eu and consequently there is no energy transfer from the ligand to the metal ion states. It was impossible to localize the LMCT state for the 1Eu monocrystal, since it is located at higher energies than those recorded for the 2Eu complex. It is probably overlapped by the intensive ligand bands, visible on the absorption spectrum taken at 295 K (see Fig. 3). The Eu(III) ion is an nine-coordinate and decacoordinate in the 1Eu and 2Eu monocrystals, respectively. For the complexes with the same ligands LMCT energies tend to increase with decreasing the coordination number [35]. For 2Eu the LMCT state lies slightly below the ligand triplet state (23,419 cm^{-1}), which makes the intramolecular energy transfer T → LMCT possible. The above said is in accordance with the theoretical analysis performed by Faustino et al. [25], where the quantum yield as a function of the relative energy position of the LMCT state is given. It is worth noting a very low intensity of usually strong [36], $^7F_0 \rightarrow {}^5D_4$, $^7F_0 \rightarrow {}^5G_J$ and $^7F_0 \rightarrow {}^5L_6$ transitions with respect

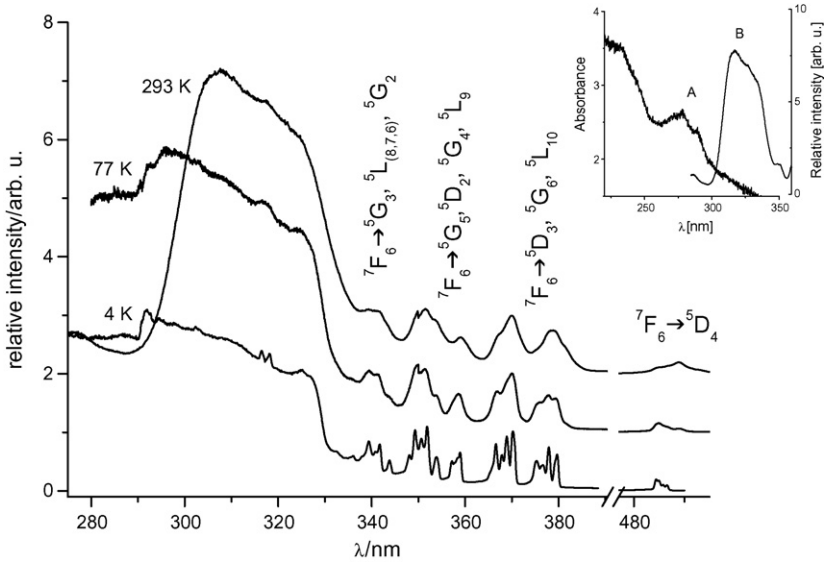

Fig. 3. The excitation spectra of 1Tb at 295, 77 and 4 K. The inset shows the excitation and absorption spectra of 1Tb taken at 295 K.

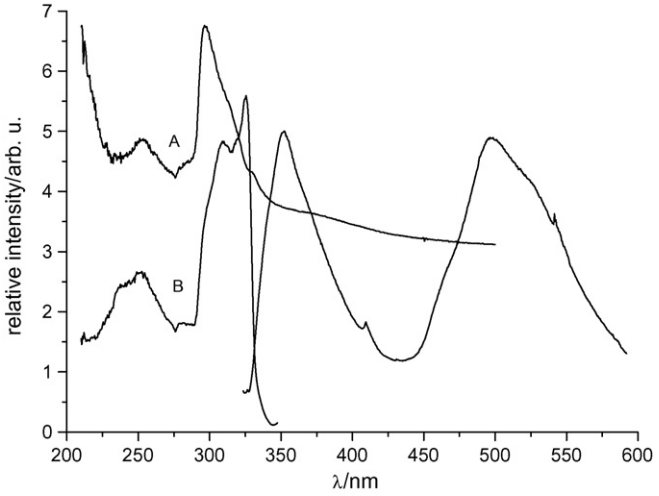

Fig. 4. The luminescence (λ_{exc} = 325 nm) and excitation spectra (λ_{mon} = 540 nm (A), λ_{mon} = 360 nm (B)) of 1Gd at 77 K.

to the $^7F_0 \rightarrow {}^5D_2$ and $^7F_0 \rightarrow {}^5D_1$ ones for 2Eu in comparison with 1Eu. This results from the resonance of the LMCT state with the $^7F_0 \rightarrow {}^5G_J$, $^7F_0 \rightarrow {}^5D_4$ and $^7F_0 \rightarrow {}^5H_J$ and $^7F_0 \rightarrow {}^5L_6$ transitions. The LMCT state was localized from the absorption spectrum at 295 K [23]. It partially depopulates the Eu(III) excited states and empties into the ^7F_J ground state manifold, resulting in strong reduction of luminescence.

In Fig. 6, we plotted the 77 K emission spectra from the $^5D_1$ level for 1Eu, 2Eu monocrystals. The presence of the $^5D_1$ emission is rather surprising, due to the presence of 3 and 2 water molecules in the inner coordination sphere, for the complexes 1Eu and 2Eu respectively. The small energy gaps between $^5D_1$ and $^5D_0$ excitation levels equal 1747 (1Eu) and 1777 (2Eu) cm^{-1} and the presence of the OH_{H20} groups with highly energetic oscillations (3600 cm^{-1}) results in a non-radiative multi-phonon relaxation from the $^5D_1$ to $^5D_0$ state. The emission from the $^5D_1$ state of Eu(III) is also controlled by the cross-relaxation process. The efficient $^5D_1$ emission in both investigated compounds shows inefficient $^5D_0 \rightarrow {}^5D_1$, $^7F_0 \rightarrow {}^7F_3$ cross-relaxation. The $^5D_1$ emission of 1Eu is accompanied by weak ligand phosphorescence. Due to the resonance between the $^5L_6$ level of Eu(III) and the ligand triplet state the excitation with 395 nm line leads to the simultaneous emission from both levels.

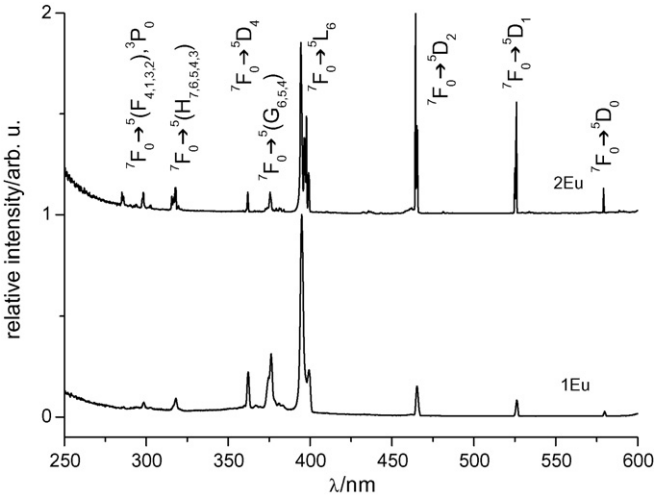

Fig. 5. The excitation spectra of 1Eu, 2Eu at 77 K.

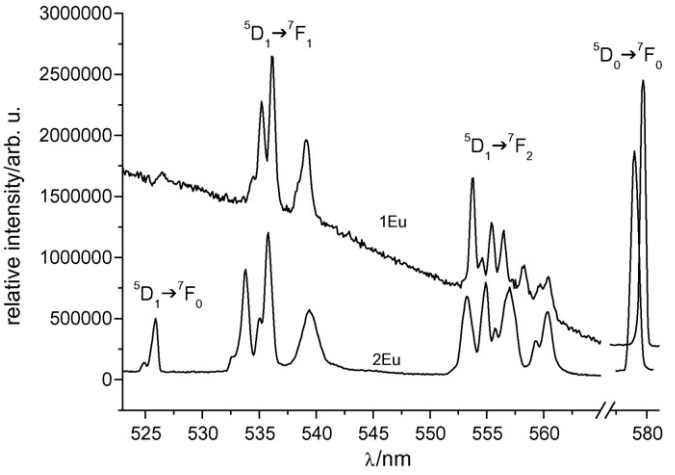

Fig. 6. The spectra of the $^5D_1$ emission of 1Eu and 2Eu at 77 K (λ_{exc} = 395 nm).

Based on the presence of this process, it may be concluded that the LMCT state in the 1 Eu complex may be localized in the vicinity of the singlet ligand state. Thus, the intramolecular energy transfer $S_1 \rightarrow$ LMCT would be possible. In those cases we have to do with two competing processes whose efficiency depends on the energy transfer rates $S_1 \rightarrow$ LMCT and $S_1 \rightarrow$ T. The ligand phosphorescence accompanying the highly temperature dependent emission from the $^5D_1$ level for 2Eu was not detected.

Fig. 7 presents the 77 K emission spectra of the 1Eu monocrystals from the $^5D_0$ levels at 295 and 77 K. The emission spectrum at 77 K for 1Eu is similar to 2Eu [23]. The number of Stark components for the $^5D_0 \rightarrow {}^7F_J$ (J = 1–4) transitions suggest that the Eu(III) occupy a low-site symmetry without an inversion centre. The presence of only one line, with half width 9 cm^{-1}, for the $^5D_0 \rightarrow {}^7F_0$ transitions for both complexes indicates the existence of only one coordination site of Eu(III) ions in the complexes with polymeric structure [11,37]. The maxima of the $^5D_0 \rightarrow {}^7F_0$ bands are located at 17,255 and 17,271 cm^{-1} for 1Eu and 2Eu, respectively. The shift of the maxima of the $^5D_0 \rightarrow {}^7F_0$ transition is attributed to the nephelauxetic effect. This shift can reflect either an increase in the metal–ligand bond covalency or a decrease in effective nuclear charge on the metal ion upon complexation. The red emission for 1Eu does not depend on the temperature, while its intensity rises strongly for 2Eu with the temperature decrease.

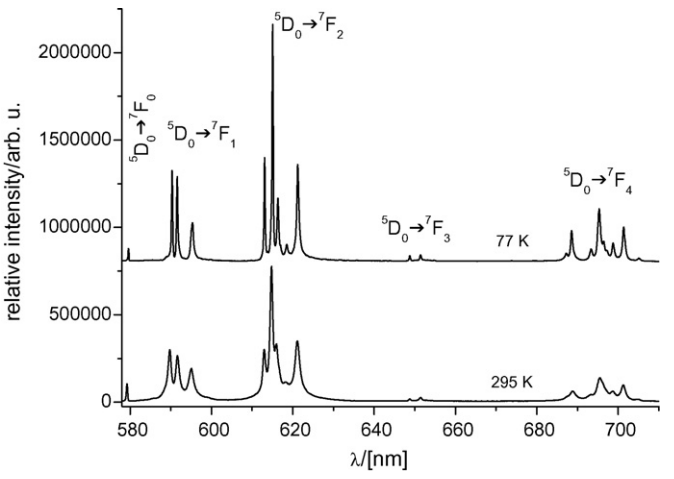

Fig. 7. The spectra of $^5D_0$ emission of 1Eu complex at 295 and 77 K (λ_{exc} = 395 nm).

Table 4
The emission decay times of $^5D_0$ level for 1Eu, 2Eu and of $^5D_4$ level for 1Tb and of $3\pi\pi^*$ ligand state for 1Gd.

	τ, μs			
	1Eu	2Eu	1Tb	1Gd
295 K	279	307	822	
77 K	281	439	895	2560

The values were estimated with error of 5%.

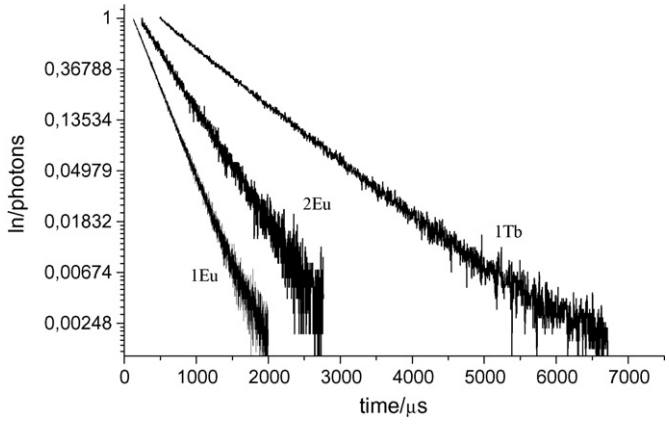

Fig. 8. Emission decay times for 1Eu, 2Eu and 1Tb at 77 K.

This is reflected in the decay time of the emission from the $^5D_0$ level, the values of which are presented in Table 4. It has to be mentioned that the value of decay times for 2Eu published in [23] was measured for derivative of PDDA and included by mistake. The emission decay times for 1Eu, 2Eu, 1Tb, 1Gd are monoexponential and do not depend on the temperature for 1Eu and 1Tb (see Fig. 8 and Table 4). The most important mechanism for the temperature-independent non-radiative relaxation is that occurring through OH vibrations. The hydration number of 1Eu was additionally calculated using the simplified equation obtained by Barthelemy and Choppin [38]:

$$n = 1.05 \times \tau^{-1} - 0.70 \quad (1)$$

This equation is true when there is no contribution from the ligand to the de-excitation of the Eu(III) excited state. The calculated number of water molecules ($n = 3.06$) is conformable to the X-ray analysis for 1Eu, proving that the LMCT state is located at higher energies then for 2Eu. Eq. (1) cannot be used to determine the number of water molecules in the innner coordination sphere of the 2Eu complex. Strong temperature dependence of the luminescence decay time of the $^5D_0$ emission level for 2Eu suggests that the LMCT state of Eu(III) takes part in a non-radiative deactivation of the excited Eu(III) levels (Table 4).

3.2.3. Tb and Eu complexes in aqueous solutions

The strong temperature dependence of the luminescence lifetime was also recorded for aqueous solution of Eu(III) with PDDA, which was reflected in $k_{nr}(T)$. The results are presented in Table 5. Measurement of the lifetimes in H_2O and D_2O solution allows to estimate the number of Eu(III) bound water molecules, n, using the following equation derived by Supkowski and Horrocks [39]

$$q = 1.11[\tau(H_2O)^{-1} - \tau(D_2O)^{-1} - 0.31] \quad (2)$$

where the lifetimes are measured at room temperature and are entered in msec. The refined equation is used to account for the effect of water molecules in the second coordination sphere of Eu(III) and is also useful for Eu(III) complexes with labile coordination spheres [39]. Substitution of the measured lifetimes into this equation yields a q value of 0.91. This result is consistent with the presence of approximately one molecule of water in the first coordination sphere or the equilibrium between two Eu(III) complexes with $q = 0$ and $q = 1$ favouring the $q = 1$ complex.

It is also possible to estimate the other temperature dependent and temperature independent parts of the non-radiative decay constants in the manner of Prodi et al. [40]. In this analysis, the overall rate constant, k, is expressed as follows

$$k = \frac{1}{\tau} = k_r + k_{nr}(T) + k_{nr}(OH) + k_{nr}\,(\text{other vibrations}) \quad (3)$$

where k_r is the radiative rate constant, $k_{nr}(T)$ is the temperature-dependent non-radiative rate constant, and it is assumed that the most important mechanism for temperature independent non-radiative relaxation ($k_{nr}(OH)$) is that achieved through high energy OH vibrations, where:

$$k_{nr}(T) = [\tau(D_2O)_{300\,K}]^{-1} - [\tau(D_2O)_{77\,K}]^{-1} \quad (4)$$

and

$$k_{nr}(OH) = [\tau(D_2O)_{300\,K}]^{-1} - [\tau(H_2O)_{300\,K}]^{-1} \quad (5)$$

Numerous papers have been based on the assumption that all possible non-radiative processes for Eu(III) ion complexes in D_2O at the temperature of 77 K may be neglected [8,21] and it was assumed that $k_r = [\tau(D_2O)_{77\,K}]^{-1}$. This is obviously a conscientious simplification and the thus obtained decay times of 2 ms are shorter than the real radiative lifetimes. West et al. have demonstrated experimentally that the radiative lifetime of the $^5D_0$ excited state of Eu(III) can be calculated directly from its corrected emission spectrum, without using Judd–Ofelt theory [18]. In their paper they have described Eq. (6), which relates the shape of the emission spectrum of Eu(III) to its radiative lifetime.

$$\frac{1}{\tau_R} = A_{MD,0} n^3 \left(\frac{I_{tot}}{I_{MD}}\right) \quad (6)$$

In this formula, n is the refractive index of the solvent, $A_{MD,0}$ is the spontaneous emission probability for the $^5D_0 \rightarrow {}^7F_1$ transition in vacuo, and I_{tot}/I_{MD} is the ratio of the total area of the corrected Eu(III) emission spectrum to the area of the $^5D_0 \rightarrow {}^7F_1$ band. The value of $A_{MD,0}$ was found to be 14.65 s^{-1} [18]. Using the above equation, we have estimated the radiative lifetime for Eu(III) ion complex with PDDA in aqeous solution. It amounts to 5.4 ms and is much longer than the decay time (1.8 ms) for this complex, measured in D_2O at a temperature of 77 K, indicating that k_{nr}(77 K) in D_2O should not be neglected.

The temperature dependent non-radiative decay rate is higher than the independent part of the non-radiative decay constant, which suggests that the LMCT states of Eu(III) might also participate in non-radiative deactivation of excited Eu(III) at room temperature. The sensitised emission of Eu(III) was observed for the complex in aqueous solution at 77 K, although the energy transfer from the ligand to the metal ion states does not exist for the 1Eu and 2Eu monocrystals. This phenomenon is rather unexpected. In particular, the emission spectra of 1Eu monocrystal and the complex in water are similar [23]. Their spectra differ in the relative intensities of the respective Stark components of the $^5D_0 \rightarrow {}^7F_2$ bands and in

Table 5
Luminescence data for Eu(III) complex with PDDA in aqueous solution. The values were estimated with error of 5%.

τ_H, μs		τ_D, μs		k_r, s^{-1}	$k_{nr}(OH)$, s^{-1}	$k_{nr}(T)$, s^{-1}	q
295 K	77 K	295 K	77 K				
251	768	351	1802	185	1137	2294	0.91

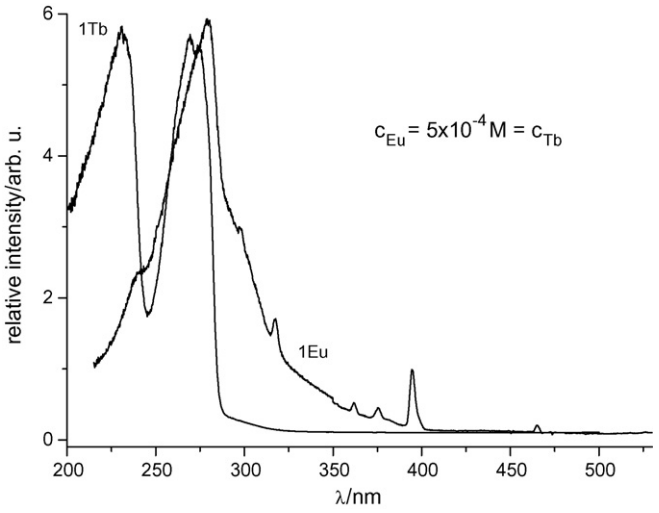

Fig. 9. The excitation spectra of Eu(III) and Tb(III) complexes with PDDA in aqueous solution at 77 K (λ_{exc} = 325 nm).

the shapes and energies of the $^5D_0 \rightarrow {}^7F_1$ transition. The presence of only one line with half width 19 cm^{-1} at 77 K for the $^5D_0 \rightarrow {}^7F_0$ transition (Fig. 9) indicates the existence of one dominating form of the complex in solution, probably ML_2. The hypersensitive transition, $^5D_0 \rightarrow {}^7F_2$, dose does not change if the Eu:L molar ratio is equal to or higher then 1:2 [24]. Taking into account that the position of the $^5D_0 \rightarrow {}^7F_0$ transitions for the 1Eu monocrystal and the complex in solution are almost identical, equalling 17,255 and 17,253 cm^{-1} respectively, it can be assumed that CN is the same for both complexes and equals 9. One water molecule is present in the first coordination sphere of the complex in solution and CN up to 9 can be completed by the two tetra dentate ligand molecules. However, the half width of the $^5D_0 \rightarrow {}^7F_0$ band and non-integral q-value would be consistent rather with differing numbers of first coordination sphere water molecules in fast exchange favouring complex with $q = 1$. The different structure of complexes influences the position of the LMCT state, which – for the complexes in solution – could be located at lower energy as compared to the 1Eu monocrystal. Moreover, the comparison of the excitation spectra for Eu(III) and Tb(III) solutions, which are shown in Fig. 9, allows to conclude that the CT state participates in the L→ Eu(III) energy transfer process in solution at 77 K. This conclusion is supported by the presence of an additional band at the spectral range of 388–314 nm, which is not observed in the Tb(III) excitation spectra.

4. Conclusions

Two investigated types of Eu(III) compounds illustrate how the complex structures, anionic $[Eu(C_{10}H_8O_6)_2(H_2O)_2]^-$ (C.N. = 10) and neutral $[Eu(C_{10}H_8O_6)_{1.5}(H_2O)_3]$ (C.N. = 9) affect the position of the LMCT state and in consequence the emission properties of the system. The ligand-to-metal energy transfer for 1Eu and 2Eu neither at 295 nor at 77 K was not observed, since in both complexes the LMCT states deactivate the ligand states by the intramolecular energy transfer T→ LMCT for 2Eu and probably also by the intramolecular energy transfer $S_1 \rightarrow$ LMCT for 1Eu. This shows the importance of the LMCT state position in relation not only to the Eu(III) excited states, but also to the excited ligand singlet and triplet states. However, the sensitised emission was observed for Eu(III) complex in aqueous solution at 77 K. Based on determined relative contribution of the radiative and non-radiative paths to the excited state deactivation it was concluded that the contribution of temperature dependent non-radiative process to quenching of the Eu(III) emission in solution was very high. The effective ligand-to-metal energy transfer was proved for 1Tb. The back-energy transfer from the $^5D_4$ level of Tb(III) to the ligand state was excluded, based on the energy gap between the ligand $3\pi\pi^*$ and $^5D_4$ states determined as 2775 cm^{-1} and the decay times at 295 and 77 K.

Acknowledgement

The authors would like to thank dr A. Szemik-Hojniak for the possibility of decay times measurements. This work was supported through a grant No. 20401331/0289 from the Polish Committee for Scientific Research.

References

[1] I.A. Hemmilä, Applications of Fluorescence in Immunoassays, Wiley, 1991; A. Hemmilä, T. Stahlberg, P. Mottram, Bioanalytical Applications of Labeling Technologies, 2nd ed., Wallac Oy, Turku, 1995; A. Hemmilä, V. Laitala, J. Fluor. 15 (2005) 529.
[2] H. Bazin, E. Trinquet, G. Mathis, Rev. Mol. Biotechnol. 82 (2002) 233.
[3] A. Beeby, S.W. Botchway, I.M. Clarkson, S. Faulkner, A.W. Parker, D. Parker, J.A.G. Williams, J. Photochem. Photobiol. B: Biol. 57 (2000) 83.
[4] V.W.W. Yam, K.K.W. Lo, Coord. Chem. Rev. 184 (1999) 157.
[5] J. Legendziewicz, E. Huskowska, Application of luminescence in studies of Ln(III) ions interaction with amino acids, in: J. Legendziewicz, W. Strek (Eds.), Excited States of Transition Elements, World Scientific Publishing Co. Pte. Ltd., Singapore, 1989, p. 222.
[6] L.J. Krick, Ann. Clin. Biochem. 39 (2) (2002) 114.
[7] J.C. Bünzli, in: A. Siegel, H. Siegel (Eds.), Metal Ions in Biological Systems, vol. 42, Marcel Dekker Inc., New York, 2004 (Chapter 2, p. 39).
[8] P. Gawryszewska, J. Sokolnicki, J. Legendziewicz, Coord. Chem. Rev. 249 (2005) 2489; P. Gawryszewska, L. Jerzykiewicz, M. Pietraszkiewicz, J. Legendziewicz, J.P. Riehl, Inorg. Chem. 39 (2000) 5365; P. Gawryszewska, J. Sokolnicki, A. Dossing, J.P. Riehl, G. Muller, J. Legendziewicz, J. Phys. Chem. A 109 (2005) 3858.
[9] J. Legendziewicz, J. Cybińska, M. Guzik, G. Boulon, G. Meyer, Opt. Mater. 30 (2008) 1655.
[10] V.F. Zolin, L. Puntus, V.I. Tsaryuk, V. Kudryashova, J. Legendziewicz, P. Gawryszewska, R. Szostak, J. Alloys Compd. 380 (2004) 279.
[11] J. Legendziewicz, J. Alloys Compd. 341 (2002) 201.
[12] V. Zolin, J. Alloys Compd. 380 (2004) 101.
[13] J.P. Riehl, G. Muller in, K.A. Gschneidner Jr., J.-C.G. Bünzli, V.K. Pecharsky (Eds.), Handbook on the Physics and Chemistry of Rare Earths, vol. 34, North-Holland Publishing Company, Amsterdam, 2005, pp. 289–357 (Chapter 220).
[14] V.I. Tsaryuk, K.P. Zhuravlev, V.E. Zolin, V. Kudryashova, J. Legendziewicz, R. Szostak, J. Appl. Spectrom. 74 (2007) 51.
[15] A.J. Wilkinson, D. Maffeo, A. Beeby, C.E. Foster, J.A.G. Williams, Inorg. Chem. 46 (22) (2007) 9438.
[16] J.C. Bünzli, C. Piguet, Chem. Soc. Rev. 34 (12) (2005) 1048.
[17] M.H.V. Werts, R.H. Woudenberg, P.G. Emmerink, R. van Gasssel, J.W. Hofstraat, J.W. Verhoeven, Angew. Chem. Int. Ed. 39 (2000) 4542.
[18] E.B. Van der Tol, H.J. van Ramesdonk, J.W. Verhoeven, F.J. Steemers, E.G. Kerver, W. Verboom, D.N. Reinhoudt, Chem. Eur. J. 4 (1998) 2315; M.H.V. Werts, R.T.F. Jukes, J.W. Verhoeven, Phys. Chem. Chem. Phys. 4 (2002) 1542.
[19] P. Gawryszewska, O.L. Malta, R. Longo, F.R.G.E. Silva, K. Mierzwicki, Z. Latajka, M. Pietraszkiewicz, J. Legendziewicz, Chem. Phys. Chem. 5 (2004) 1.
[20] G.F. de Sá, O. Malta, C. de Mello Donega, A.M. Simas, R.L. Longo, P.A. Santa-Cruz, E.F. da Silva, Coord. Chem. Rev. 196 (2000) 165.
[21] N. Sabbatini, M. Guardigli, J.-M. Lehn, Coord. Chem. Rev. 123 (1993) 201.
[22] S. Petoud, J.-C.G. Bünzli, T. Glanzman, C. Piguet, Q. Xiang, R.P. Thummel, J. Lumin. 82 (1999) 69.
[23] P. Gawryszewska, J. Legendziewicz, J. Lumin. 122–123 (2007) 496.
[24] O.L. Malta, F. Goncalves e Silva, R. Longo, Chem. Phys. Lett. 307 (1999) 518; O.L. Malta, F. Goncalves e Silva, Spectrochim. Acta Part A 54 (1998) 1593.
[25] W.M. Faustino, O.L. Malta, G.F. de Sá, J. Chem. Phys. 122 (2005) 054109; W.M. Faustino, O.L. Malta, G.F. de Sá, Chem. Phys. Lett. 429 (2006) 595.
[26] D.M. Bassani, J.M. Lehn, G. Baum, D. Fenske, Angew. Chem. Int. Ed. Engl. 36 (1997) 1845; R.S. Dickins, J.A.K. Howard, J.M. Moloney, D. Parker, R.D. Peacock, G. Siligardi, Chem. Commun. 1997 (1747); L. Wu, T. Cheung, C. Che, K. Cheung, M.H.W. Lam, Chem. Commun. (1998) 1127.
[27] G.M. Sheldrick, Acta Crystallogr. A46 (1990) 467–473.
[28] G.M. Sheldrick, SHELXL97 Program for Crystal Structure Refinement, University of Göttingen, 1997.
[29] H.B. Kerfoot, G.R. Choppin, T.J. Kistenmacher, Inorg. Chem. 18 (1979) 787.
[30] G. Blasse, G.J. Dirksen, N. Sabbatini, S. Perathoner, J.-M. Lehn, B. Alpha, J. Phys. Chem. 92 (1988) 2419; J. Sokolnicki, J. Legendziewicz, G. Muller, J.P. Riehl, Opt. Mater. 27 (2005) 1529.

[31] S. Jockusch, G. Dedola, G. Lem, N.J. Turro, J. Phys. Chem. 103 (1999) 9126.
[32] E. Huskowska, I. Turowska-Tyrk, J. Legendziewicz, J.P. Riehl, New J. Chem. 26 (2002) 1461.
[33] M. Latva, H. Takalo, V.-M. Mukkala, C. Matachescu, J.C. Rodriguez-ubis, J. Kankare, J. Lumin. 75 (1997) 149.
[34] O.L. Malta, J. Lumin. 71 (1997) 229.
[35] H.E. Hoefdraad, J. Solid State Chem. 15 (1975) 175;
G. Blasse, Struct. Bond. 26 (1976) 43;
L. van Pieterson, A. Meijerink, J. Alloys Compd. 300–301 (2000) 426.
[36] P.P. Gawryszewska, L. Jerzykiewicz, P. Sobota, J. Legendziewicz, J. Alloys Compd. 300–301 (2000) 275.
[37] J. Legendziewicz, Spectroscopy of dimeric and polymeric Ln(III) compounds single crystals, in: J. Legendziewicz, W. Strek (Eds.), Excited States of Transition Elements, World Scientific Publishing Co. Pte. Ltd., Singapore, 1991, p. 149.
[38] P.P. Barthelemy, G.R. Choppin, Inorg. Chem. 28 (1989) 3354.
[39] R.M. Supkowski, W.D. Horrocks Jr., Inorg. Chim. Acta 340 (2002) 44.
[40] L. Prodi, M. Maestri, V. Balzani, J.-M. Lehn, C. Roth, Chem. Phys. Lett. 180 (1991) 45.